Journal of Physics: Conference Series

Microstructure and magnetoresistance of $Co_{90}Fe_{10}$/Cu and $Co_{65}Fe_{26}Ni_9$/Cu multilayers

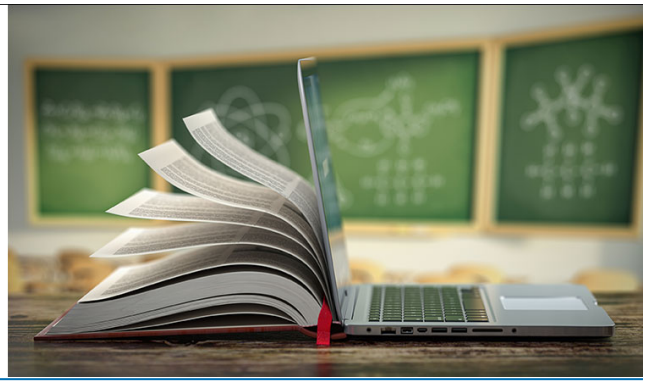

Journal of Physics: Conference Series **1389** (2019) 012156 doi:10.1088/1742-6596/1389/1/012156

Microstructure and magnetoresistance of $Co_{90}Fe_{10}$/Cu and $Co_{65}Fe_{26}Ni_9$/Cu multilayers

M A Milyaev[1, 2], L I Naumova[1, 2], N S Bannikova[1], V V Proglyado[1], E I Patrakov[1], T P Krinitsina[1] and V V Ustinov[1, 2]

[1] M.N. Miheev Institute of Metal Physics of UD of RAS, 620108, Ekaterinburg, S. Kovalevskaya st., 18, Russia
[2] Ural Federal University, INSM, 620002, Ekaterinburg, Mira st., 19, Russia

E-mail: milyaev@imp.uran.ru

Abstract. Investigations of the microstructure, magnetic and magnetotransport properties of the optimized $[Co_{90}Fe_{10}/Cu]_n$ and $[Co_{65}Fe_{26}Ni_9/Cu]_n$ multilayers with n = 32 prepared by magnetron sputtering are performed. These nanostructures exhibit the magnetoresistance values 83 % and 36 % at room temperature, respectively. The article presents the results of the influence of $Co_{65}Fe_{26}Ni_9$ alloy on the magnetoresistance values and crystal structure of multilayers. In the periodic part of the nanostructure $[Co_{65}Fe_{26}Ni_9/Cu]_n$ based on CoFeNi ternary alloy, besides fcc the formation of a bcc phase in the continuous boundaries around crystallites is found.

1. Introduction

Generally, multilayers with the giant magnetoresistive effect (GMR) are used as magnetically sensitive elements in various spintronics devices. Multilayers are artificially created materials, those magnetic and magnetotransport properties can be varied over a wide range by selecting the type of material, the thickness of the ferromagnetic (FM) and non-magnetic layers forming the nanostructure [1]. In particular, the type and thickness of the buffer layer change the magnetoresistive properties of multilayers $[FM/Cu]_n$, where FM is a ferromagnetic layer [2].

It is known that the GMR in $[FM/Cu]_n$ nanostructures can be observed only for a Cu spacer thicknesses corresponding to antiferromagnetic (AFM) interlayer exchange coupling between the neighboring FM layers. Actually, the first, second and third AFM peaks of oscillations can be observed. The values of magnetoresistance (MR) and magnetic saturation field of multilayers are oscillating when the interlayer Cu thickness is varied [1].

When comparing the multilayers with the thickness of the copper layer corresponding to the first, second and third AFM peaks, the following features are identified. The multilayers at the first AFM peak have the highest magnetoresistance and the lowest sensitivity to a magnetic field. Therefore, this type of nanostructure can be used in sensors, where it is important to measure the signal in the wide range of magnetic fields.

For the $Co_{90}Fe_{10}$/Cu multilayers with the number of bilayers n = 32 the authors of [3] obtained one of the highest values of the GMR effect, $\Delta R/R_s$ = 83%, at room temperature as a current passes through the film plane. As the temperature decreases to helium temperatures the magnetoresistance was higher than 160%.

The magnetoresistance value for multilayers at second AFM peak is smaller than for multilayers at the first AFM peak but the sensitivity to the magnetic field is the maximal one.

An important task is the search for new ferromagnetic alloys in order to obtain GMR multilayers with the highest magnetoresistance and at the same time the lowest hysteresis. For example, the ferromagnetic CoFeNi thin films show excellent soft magnetic properties and high saturation magnetization [4]. The CoFeNi alloys are used to produce GMR multilayers with a comparatively high magnetic field sensitivity of about 0.3%/Oe [5]. At the same time for this class of nanostructures the low magnetic saturation fields and weak hysteresis are obtained [5, 6].

In the recent paper [6] it was shown that the magnetoresistance of CoFeNi/Cu multilayers with different ferromagnetic layers compositions could exceed 30% at room temperature, which is comparable with the values of magnetoresistance for CoFe/Cu. It should also be noted that CoFeNi alloys possess almost a zero magnetostriction constant [7]. The multilayers based on CoFeNi alloys of the following composition: $Co_{85}Fe_{12}Ni_3$, $Co_{77}Fe_{17}Ni_6$, $Co_{70}Fe_{20}Ni_{10}$ with close high saturation magnetization values ($M_s \approx 180$ emu/g) were used. Aforementioned data were obtained for the multilayers with the thicknesses of copper layers corresponding to the second peak of the AFM oscillations.

In the ternary diagram for bulk materials, these CoFeNi alloys are in the region of a mixture of fcc and bcc phases. The threshold value of Fe for transition between these two phases is about 30% [8].
For the studied multilayer systems an fcc structure with sharp uniaxial <111> texture [2, 3, 5, 6, 9] is dominated. Nevertheless, the increasing of iron content in CoFeNi/Cu multilayers also leads to appearance of bcc phase at some value of Fe different from that for bulk materials [7].

That is why the $Co_{65}Fe_{26}Ni_9$ ternary alloy with a composition close to transition to the bcc phase was chosen for our study. Moreover, as it was shown in [6], the large magnetoresistance of up to 30% can be obtained in the CoFeNi/Cu multilayers at the second AFM peak. We supposed that the high values of MR can be also achieved for CoFeNi/Cu at the first antiferromagnetic peak with saving the weak hysteresis in nanostructure.

Therefore, in this paper the influence of $Co_{65}Fe_{26}Ni_9$ alloy on microstructure, magnetic and magnetoresistive properties of the CoFeNi-based multilayers was investigated. The step further in investigation of the role phase mixing in the GMR-multilayers was performed. The causes of low MR in synthesized $[Co_{65}Fe_{26}Ni_9/Cu]_{32}$ multilayers were also clarified.

2. Experimental details

The glass//Ta(5)/$Ni_{48}Fe_{12}Cr_{40}$(5)/$[Co_{90}Fe_{10}(1.5)/Cu(0.95)]_{32}$/Ta(5) and glass//Ta(5)/$Ni_{48}Fe_{12}Cr_{40}$(5)/$[Co_{65}Fe_{26}Ni_9(1.5)/Cu(0.9)]_{32}$/Ta(5) multilayered thin-film nanostructures were sputtered at room temperature by DC magnetron sputtering from targets of corresponding alloys. Lately it will be denote as $Co_{90}Fe_{10}$/Cu and $Co_{65}Fe_{26}Ni_9$/Cu samples, respectively.

The bilayer Ta/$Ni_{48}Fe_{12}Cr_{40}$ was used in CoFe/Cu and CoFeNi/Cu as the buffer layer. The thickness and composition of buffer layer, the thickness of copper layers and ferromagnetic layers, as well as the number of bilayers were selected according to the results of our previous papers [3, 5, 6, 9].

The studies of microstructure and texture of the samples were carried out by XRD (θ - 2θ and ω - scans) and TEM microscopy measurements. The electrical resistance of the samples was measured by the four-probe method in current-in-plane geometry at room temperature. The magnetoresistance was found as $\Delta R/R_s = [(R(H) - R_s)/R_s]\cdot 100\%$, where $R(H)$ is the electrical resistance of the sample in magnetic field H and R_s is the electrical resistance in the saturation magnetic field H_s.

The surface morphology scans (AFM) and magnetic images (MFM) were received by means of Solver Next scanning probe microscope.

3. Results and discussion

The Figure 1 shows the field dependencies of the magnetoresistance of the $Co_{90}Fe_{10}$/Cu and $Co_{65}Fe_{26}Ni_9$/Cu multilayers. For a $Co_{90}Fe_{10}$/Cu multilayer, the magnetoresistance is the largest.

According to [6], the magnetoresistance of the $Co_{85}Fe_{12}Ni_3$/Cu, $Co_{77}Fe_{17}Ni_6$/Cu and $Co_{70}Fe_{20}Ni_{10}$/Cu multilayers at the second antiferromagnetic maximum can exceed 30% at room temperature.

It means that for CoFeNi/Cu nanostructures with copper thickness t_{Cu} = 0.9-0.95 nm, one should also expect magnetoresistance values close to those obtained for CoFe/Cu.

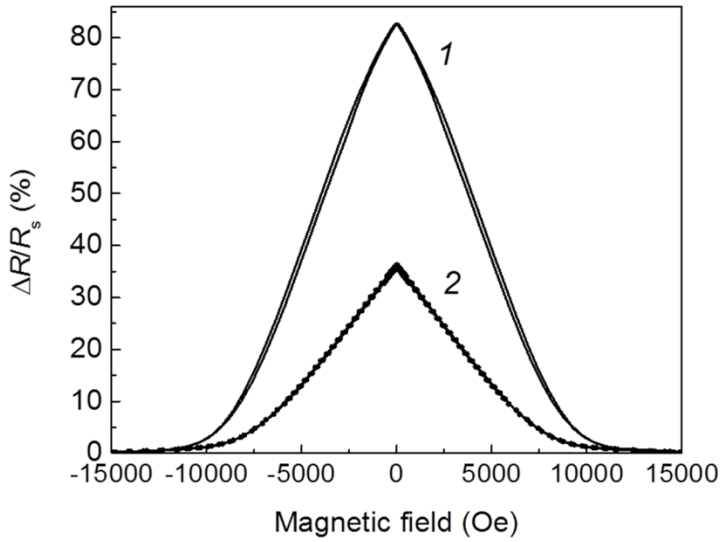

Figure 1. Field dependencies of the magnetoresistance of Ta(5)/NiFeCr(5)/[FM(1.5)/Cu(0.95)]$_{32}$/Ta(5) multilayers with FM: (*1*) – $Co_{90}Fe_{10}$ and (*2*) – $Co_{65}Fe_{26}Ni_9$.

For example, for $Co_{70}Fe_{20}Ni_{10}$/Cu with n = 24, we obtained the magnetoresistance value $\Delta R/R_s$ = 62% [10]. Compared with the above-mentioned $Co_{70}Fe_{20}Ni_{10}$ alloy, $Co_{65}Fe_{26}Ni_9$ alloy contains more Fe and shows excellent soft magnetic properties and higher saturation magnetization (M_s = 186 emu/g). However the $Co_{65}Fe_{26}Ni_9$/Cu multilayer exhibits much smaller magnetoresistance than the $Co_{90}Fe_{10}$/Cu multilayer, $\Delta R/R_s$ = 36% (Figure 1).

According to [8], $Co_{70}Fe_{20}Ni_{10}$ and $Co_{65}Fe_{26}Ni_9$ alloys are close on a ternary phase diagram in a region characterized by the coexistence of fcc and bcc phases. The X-ray diffraction (XRD) studies of a target of the $Co_{65}Fe_{26}Ni_9$ alloy show that peaks from bcc and fcc phases are presented (Figure 2). Meanwhile, the $Co_{90}Fe_{10}$ alloy has an fcc structure.

Figure 3 shows XRD patterns obtained for the (*1*) $Co_{90}Fe_{10}$/Cu and (*2*) $Co_{65}Fe_{26}Ni_9$/Cu multilayers.There is only a one peak, which is the result of diffraction X-rays from a family of planes (111) fcc structure. This peak is common to the Cu and CoFe (or Cu and CoFeNi) materials due to the proximity of their lattice parameters.

The absence of other structural peaks of the fcc lattice is due to the fact that in the multilayers an uniaxial <111> texture have been formed.

The inset Figure 3 shows the corresponding rocking curves. The full width at half height rocking curve (γ) gives estimations of the degree of perfection of the <111> texture: (*1*) γ = 2.5°, (*2*) γ = 2.0°. More perfect <111> texture was formed for $Co_{65}Fe_{26}Ni_9$/Cu in comparison to $Co_{90}Fe_{10}$/Cu multilayer. Both multilayers have a polycrystalline fcc structure and a perfect uniaxial <111> texture that is typical of these multilayers [3, 5, 6]. According to the XRD data, no differences or features in the crystal structure of the samples are revealed.

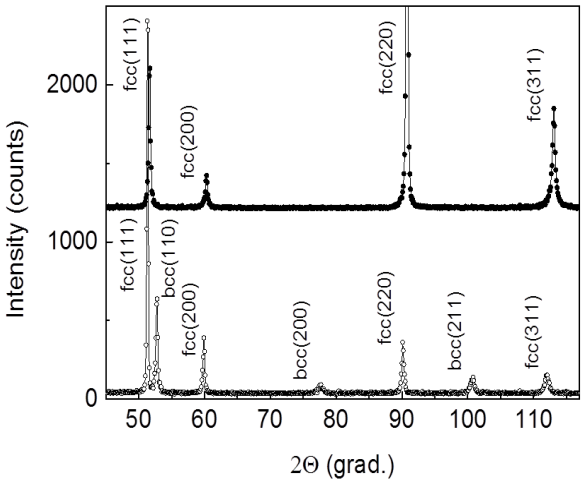

Figure 2. XRD patterns obtained for the targets of $Co_{90}Fe_{10}$ alloy and $Co_{65}Fe_{26}Ni_9$ alloy (black symbols and empty symbols, respectively).

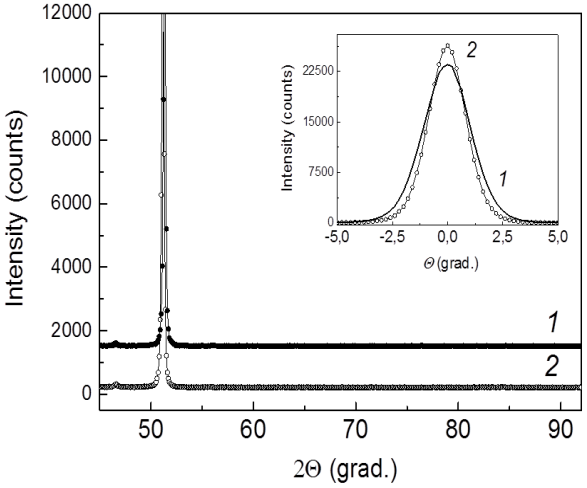

Figure 3. XRD patterns obtained for the (*1*) $Co_{90}Fe_{10}$/Cu and (*2*) $Co_{65}Fe_{26}Ni_9$/Cu multilayers. The inset shows the corresponding rocking curves.

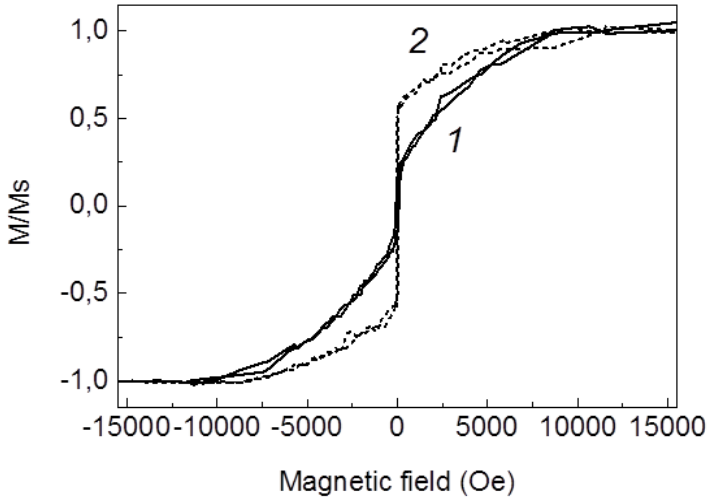

Figure 4. In-plane hysteresis loops of (*1*) $Co_{90}Fe_{10}$/Cu and (*2*) $Co_{65}Fe_{26}Ni_9$/Cu multilayers.

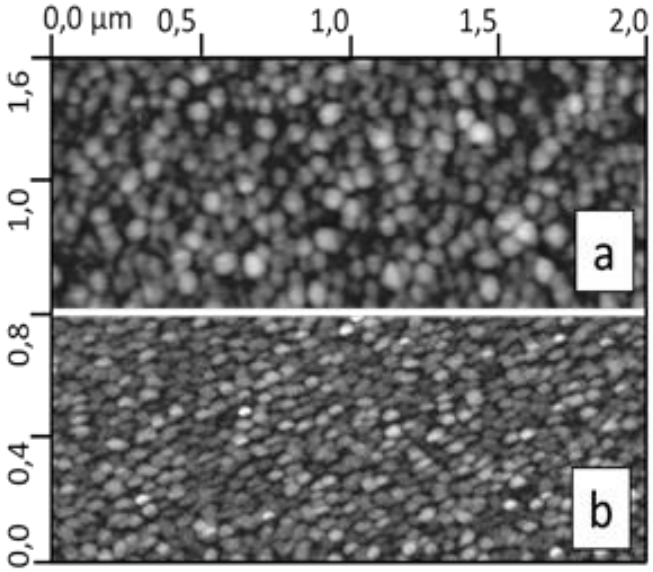

Figure 5. The surface morphology (0.8×2 µm^2) of multilayers (a) $Co_{90}Fe_{10}$/Cu and (b) $Co_{65}Fe_{26}Ni_9$/Cu.

The investigated CoFe/Cu and CoFeNi/Cu multilayers have the similar electrical resistivity values 34 and 32 (µΩ cm), respectively.

The hysteresis loops corresponding to the two studied samples are presented in Figure 4. There is a correlation between magnetic and magnetoresistive data (Figure 1, Figure 4).

Figure 5 shows the surface AFM scans of two samples. It can be seen that the morphology of surfaces is slightly different. For (a) CoFe/Cu an average surface grain size is equal 80 nm, for (b) CoFeNi/Cu the grains are elongated and an average size is equal 45 nm. The root-mean-square Rms roughness of the samples surface is 0.5 nm and 1.0 nm, respectively. Despite the fact that both samples are deposited onto substrates with the same surface roughness and have the same buffer and protective layer, the CoFe/Cu multilayer is smoother than the CoFeNi/Cu one. In general, the larger roughness – the more interfacial defects and areas of ferromagnetic coupling in a multilayer.

The results of the magnetic force imaging experiments are shown in Figure 6. The MFM images have been recorded simultaneously along with AFM images. As can be seen from the Figure 6, for both samples the magnetic nonuniformity is observed. This nonuniformity can be classified as ripple structure and reflects the irregular polycrystalline nature of the films [11]. The images (a) and (b) are presented in one XYZ scale, so it can be concluded that the ripple structure in the CoFeNi/Cu sample is more pronounced, while in CoFe/Cu is less. The system of magnetic domains under certain conditions evolves out of an incipient ripple structure [11]. This is in good agreement with the magnetic data (Figure 4).

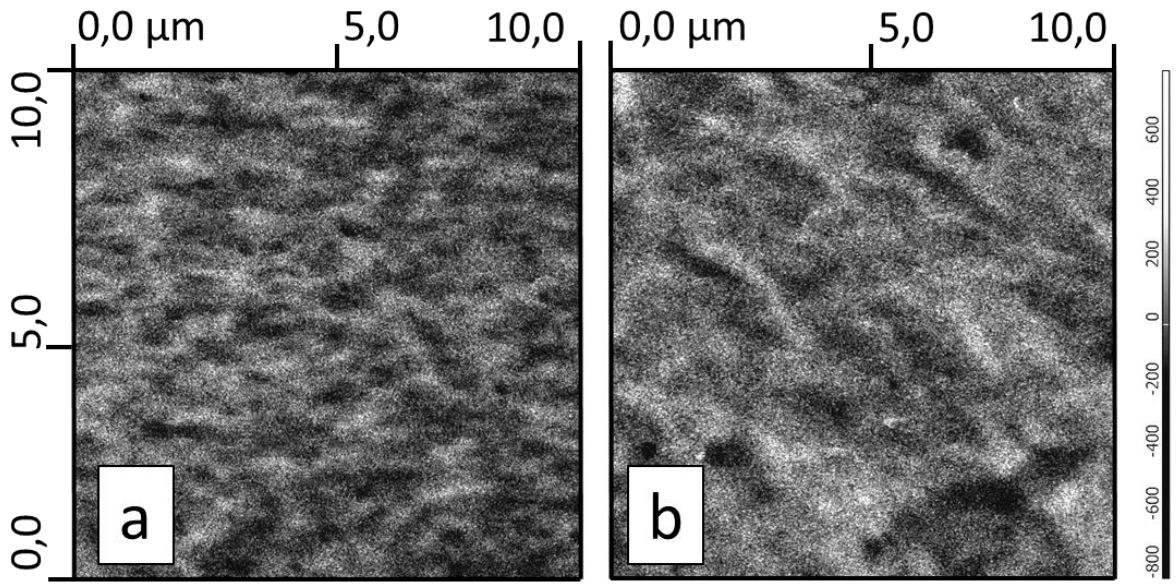

Figure 6. The MFM images (10×10 µm^2) of multilayers (a) $Co_{90}Fe_{10}$/Cu and (b) $Co_{65}Fe_{26}Ni_9$/Cu.

The results of TEM investigation revealed some essential differences in microstructure of the studied multilayers (Figure 7). The patterns are very similar to each other. The obtained spot-like reflections are characteristic of block single crystals with a small angular disorientation. The materials in the periodic structure and in buffer layer ($Co_{90}Fe_{10}$, $Co_{65}Fe_{26}Ni_9$, Cu and $(Ni_{80}Fe_{20})_{60}Cr_{40}$) have very close parameters of fcc lattice. Thus, in both electron diffraction patterns there are reflections, which form a network of large equilateral triangles. This arrangement of the reflections coincides with the standard network displaying the [111] direction in fcc crystal is parallel to the electron beam. This orientation of crystallites is characteristic of the ⟨111⟩ texture with the axis perpendicular to the film plane.

It is significant that in both patterns there are the reflections, which demonstrate another characteristic arrangement. It is a network of small equilateral triangles. This standard network refers to bcc crystal and displays the [111] direction that is parallel to the electron beam. It can be seen that the diffraction patterns of both multilayers are nearly identical, but their microstructures are different. Thus, two structural phases with close parameters exist in the both multilayers: fcc and bcc.

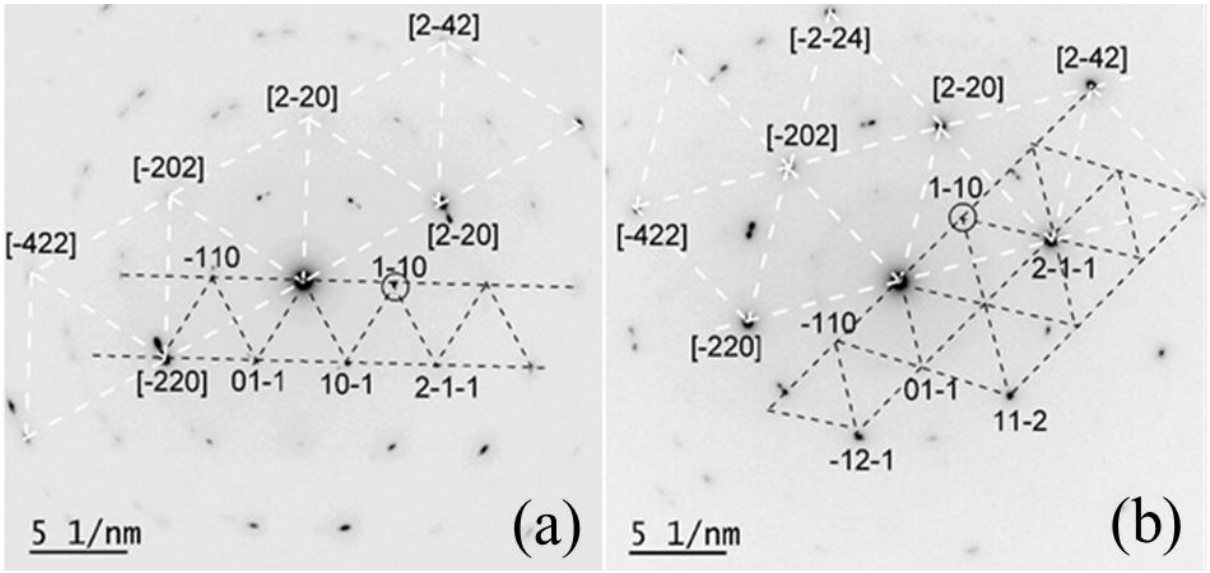

Figure 7. Electron diffraction patterns of the multilayers $Co_{90}Fe_{10}$/Cu (a) and $Co_{65}Fe_{26}Ni_9$/Cu (b). White and black dash lines refer to fcc and bcc network of triangles. Square frames indicate the fcc reflections.

What is the distribution of these phases in the microstructure? The dark-field image (Figure 8) taken in the (1-10) reflection of bcc (the reflection is noted by circle in Figure 7) indicates bright areas corresponding to crystallites with the formed bcc structure.

For the $Co_{65}Fe_{26}Ni_9$/Cu multilayer the bcc phase surrounds the crystallites like the continuous border. In the case of CoFe/Cu there is no such accurate distribution of a bcc phase on borders of crystal grains and the amount of the phase is less.

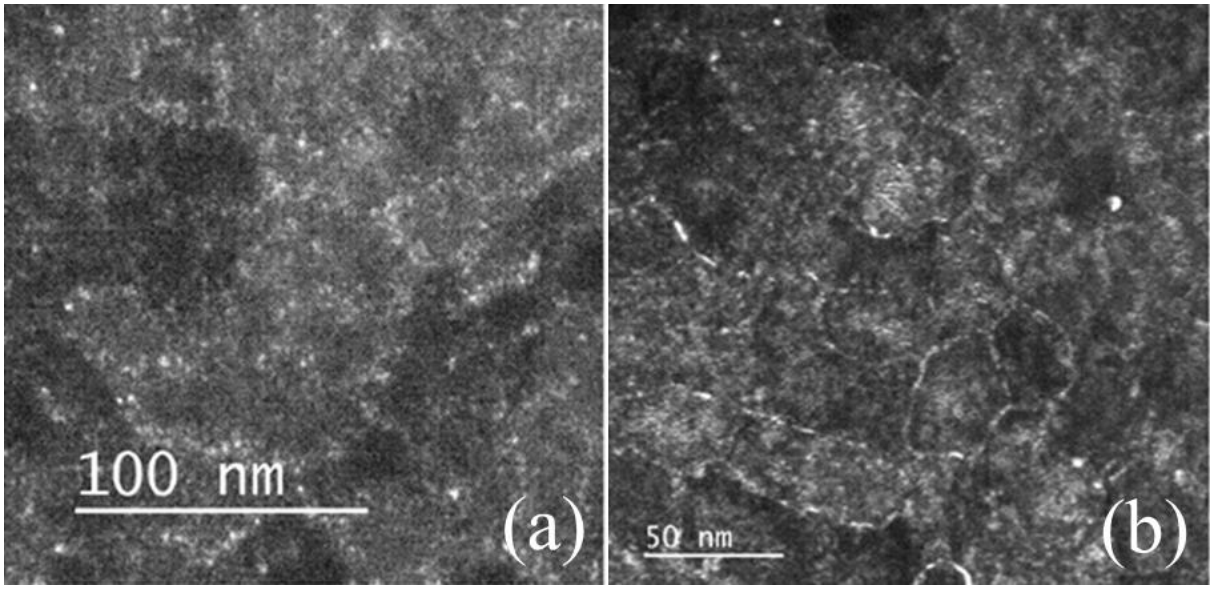

Figure 8. Dark-field images in (1-10) reflection of a cross section TEM image of the multilayers $Co_{90}Fe_{10}$/Cu (a) and $Co_{65}Fe_{26}Ni_9$/Cu (b).

It may well be that in CoFe/Cu multilayer a bcc structure appears in Ta/$(Ni_{80}Fe_{20})_{60}Cr_{40}$ buffer layer only, as it was reported in paper [5]. As it was shown earlier (Figure 2) the bulk $Co_{65}Fe_{26}Ni_9$ alloy

target has both fcc and bcc phases. Thus, it is possible that the bcc phase in the periodic part of the $Co_{65}Fe_{26}Ni_9$/Cu nanostructure is formed.

It is clear from TEM images (Figure 8) that bcc phase concentrates in the borders around crystallites. We suppose that such arrangement of $Co_{65}Fe_{26}Ni_9$ bcc phase is the reason of magnetic nonuniformity of the CoFeNi/Cu multilayer because of the significant difference in saturation magnetization of bcc and fcc phases. This nonuniformity leads to lower value of magnetoresistance for the $Co_{65}Fe_{26}Ni_9$/Cu multilayer.

4. Conclusion

We compared magnetic, magnetotransport and structural properties of two multilayers based on $Co_{90}Fe_{10}$ and $Co_{65}Fe_{26}Ni_9$ ferromagnetic alloys. Optimization performed in multilayers allowed obtaining the maximum values of magnetoresistance of about 83% for the $Co_{90}Fe_{10}$/Cu and about 36% for the $Co_{65}Fe_{26}Ni_9$/Cu multilayers.

By summarizing the experimental TEM and XRD data we deduced that the lower MR for $Co_{65}Fe_{26}Ni_9$/Cu is caused by the formation of continuous bcc boundary phase around the fcc phase crystallites in the periodic part of the nanostructure. It is important that these structural features were observed by TEM investigation only. The XRD data were similar to both multilayers showing only the fcc structure with a sharp uniaxial <111> texture.

The bcc phase in $Co_{65}Fe_{26}Ni_9$ can be also responsible for the magnetic nonuniformity of the multilayer due to the substantial difference in the saturation magnetization of the bcc and fcc phases. As a result, there has been the reduction of magnetoresistance in $Co_{65}Fe_{26}Ni_9$/Cu multilayers detected.

Acknowledgments

This work was supported in part by the State Assignment on the Theme "Spin" (Grant AAAA-A18-118020290104-2), in part by the RFBR (Grant 19-02-00057) and in part by the Integrated Program of UB RAS (Grant 18-10-2-37).

The investigations of microstructure were performed in Collaborative Access Center "Testing Center of Nanotechnology and Advanced Materials" of M. N. Miheev Institute of Metal Physics of the Ural Branch of the Russian Academy of Sciences.

5. References

[1] *Handbook of Spintronics*, 2016 ed. by Xu Y. [et al.]. (New York, London: Springer Science+Business, Media Dordrecht)
[2] Milyaev M A, Naumova L I, Proglyado V V, Krinitsina T P, Burkhanov A M, Bannikova N S, Ustinov V V 2011 *Phys. Met. Metallogr.* **112** 138
[3] Milyaev M, Naumova L., Proglyado V, Krinitsina T, Bannikova N, Ustinov V V 2019 *IEEE Trans. Magn.* **55** 2300904
[4] Kim Y M, Choi D, Kim S R, Kim S R, Kim S R, Han S H, Kim H J 2001 *JMMM* **226–230** 1507
[5] Bannikova N S, Milyaev M A, Naumova L I, Krinitsina T P, Patrakov E I, Proglyado V V, Chernyshova T A, Ustinov V V 2016 *Phys. Sol. Stat.* **58** 2011
[6] Milyaev M A, Bannikova N S, Naumova L I, Proglyado V V, Patrakov E I, Kamenskii I Yu, Ustinov V V 2019 *Phys. Met. Metallogr.* **120**, 905
[7] Miyazaki T., Oomori T., Sato F., Ishio S. 1994 *JMMM* **129** L135
[8] Scheunert G, Heinonen O, Hardeman R, Lapicki A, Gubbins M, Bowman R M 2016 *Appl. Phys. Rev.* **3** 011301
[9] Bannikova N S, Milyaev M A, Naumova L I, Proglyado V V, Krinitsina T P, Kamenskii I Yu, Ustinov V V 2015 *Phys. Met. Metallogr.* **116**, 987
[10] Will be published elsewhere.
[11] Hubert A, Schäfer R 1998 *Magnetic Domains. The Analysis of Magnetic Microstructures* (Berlin, Heidelberg: Springer-Verlag)